



Effect of Maximum Piston Velocity on Internal Homogeneity of AlSi9Cu3(Fe) Alloy Processed by High-Pressure Die Casting

M. Matejka^{a, *} , D. Bolibruchová^a , R. Podprocká^b

^aUniversity of Zilina, Faculty of Mechanical Engineering, Department of Technological Engineering, Slovak Republic

^bRosenberg-Slovakia s.r.o., Slovak Republic

* Corresponding author. E-mail address: marek.matejka@fstroj.uniza.sk

Received 31.05.2022; accepted in revised form 14.09.2022; available online 08.12.2022

Abstract

High-pressure die casting results in a high quality surface and good mechanical properties of castings. Under the effect of pressure, integral and solid castings are achieved without a large number of foundry defects. The correct and proper setting of technological parameters plays a very important role in minimizing casting defects. The aim of the presented article is to determine the optimum maximum piston velocity for a casting in the high-pressure casting process with two height variants, depending on their internal quality. It is because the internal quality of particular castings is important in terms of proper functionality in operations where the biggest problem is the porosity of the casting. The main cause of porosity formation is the decreasing solubility of gases (most often hydrogen) during the melt solidification. Solubility represents the maximum amount of gas that can dissolve in a metal under equilibrium conditions of temperature and pressure. Macroporosity and microporosity were determined from the sections of the surfaces in the determined zones of the castings. Here, the results was that the macroporosity decreased with increasing piston velocity. Ideal microstructure was evaluated at a piston velocity of 3 m/s for both types of castings. On the other hand, the increase in tube size has shown that velocities of 3 m/s and higher, the tube is more prone to macroporosity formation. The highest hardness was achieved at the piston velocity of 2 m/s at both tube lengths.

Keywords: Al-Si-Cu alloy, High-pressure die casting, Porosity, Brinell hardness, Microstructure

1. Introduction

High-pressure die casting of aluminum alloys using a machine with a cold vertical chamber has over time become one of the most used and most economical technologies. This method has become attractive especially in the manufacture of shape-complex, dimensionally accurate and thin-walled castings. [1,2].

High-pressure casting is a considerably complex process, which involves many factors that significantly affect the final state of the casting. It is possible to minimize defects in castings,

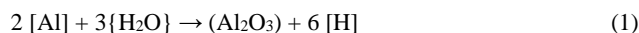
for example by changing the technological parameters of the process, by modifying the casting design or by a combination of both [3-5]. The basic parameters of the high-pressure casting process include mainly the holding temperature, the temperature of casting and the mold, the hydrostatic pressure or the pressing pressure, or the flow velocity of the alloy in the inlet notch [6].

The pressing velocity in the filling chamber determines the flow velocity of the melt in the gating system and the gate. The flow velocity of the melt in the gate then defines the filling mode of the mold cavity, which is an important factor from which the surface and internal quality of the casting is derived. Higher



numbers of smaller-sized bubbles located in the central region of the casting are characteristic of the higher filling velocities by a turbulent-dispersive flow of the melt. When filling at lower filling velocities, a reverse turbulent asymmetric flow was formed with a small number of larger vortices in the central regions. These central regions are characterized by the presence of a smaller number of bubbles together with relatively unaffected regions [7-9]. In general, the flow velocity in the gate is selected in the range from 0.6 to 100 m/s. Low velocities can lead to misrun of castings or cold shut formation. Exceeding the optimum flow velocity causes the melt flow to strike the walls of the mold cavity with high kinetic energy. This washes away the initially formed crust into the interior of the casting wall and a causes the alloy to stick on the mold wall, which results in a map-like surface of the casting due to the diffusion of the melt elements into the overheated wall of the high-pressure mold [10-11].

The most harmful gases for aluminum alloys are hydrogen, oxygen and water steam. They get into the mold from the atmosphere, the lining of the furnace, crucibles and tools. When the molten metal comes in contact with water steam, water dissociation occurs. Oxygen reacts with aluminum, hydrogen dissolves in the molten metal. The reaction proceeds according to the following equation:



Another significant source of hydrogen can be charge material if it is added to the melt without thorough preheating. Hydrogen is bound in the form of water in the pores, and in the form of hydroxides on the oxidized surface in the form of $\text{Al}(\text{OH})_3$ [12-13].

The aim of the presented article is to determine the effect of piston velocity during mold filling in high-pressure casting with two height variants, depending on their internal quality. Porosity, hardness and microstructure are important characteristics that have a direct impact on the overall quality of the high-pressure casting and its proper functionality in service. The maximum velocity of movement of the piston in the filling chamber is one of the basic technological factors in the high-pressure casting process, but its influence on internal quality such as porosity, hardness or microstructure is still not fully understood.

2. Experimental process

The castings used for experimental purposes are shown in Figure 1. Experimental castings were cast from sub-eutectic aluminum alloy $\text{AlSi9Cu3}(\text{Fe})$, which is characterized by high thermal and chemical resistance and good strength. The chemical composition of the alloy used is given in Table 1.

Table 1.
Chemical composition of the $\text{AlSi9Cu3}(\text{Fe})$ alloys [wt.%]

Si	Fe	Cu	Mn	Mg	Cr	Ni	Zn
10.3	0.72	2.1	0.16	0.13	0.02	0.07	0.6

The castings used in the experimental part were cast in the company Rosenberg-Slovakia s.r.o., Medzev, in cooperation with

the Department of Technological Engineering of the University of Žilina.

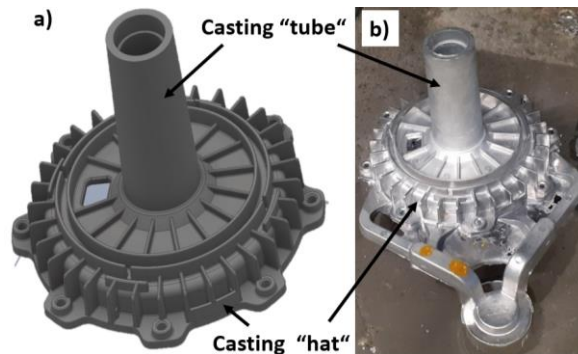


Fig. 1. Geometry of casting Statorbuchse GD 150

Castings marked Statorbuchse GD 150 were cast in two tube height variants (Statorbuchse GD 150/120 and Statorbuchse GD 150/85), while the hat part remained unchanged. The change in the specific dimensions of the length of the tube is shown in Figure 2. Both types of castings were cast in four alternatives, with a change in the maximum velocity of the press piston in the filling chamber v_{max} or the mold filling velocity. The change of casting speeds was performed during the second stage of filling with the piston. During the 1st and 3rd stages of filling we maintained the constant velocity or the maximum pressure in the chamber at each casting process. Other parameters of the machine (such as mold temperature, casting temperature and active chamber length) remained unchanged as well during the casting process (Table 2) and were taken over from Rosenberg-Slovakia s.r.o. The maximum speeds of the press piston in the casting process were chosen from 2 to 4 m/s and are presented in Table 3.

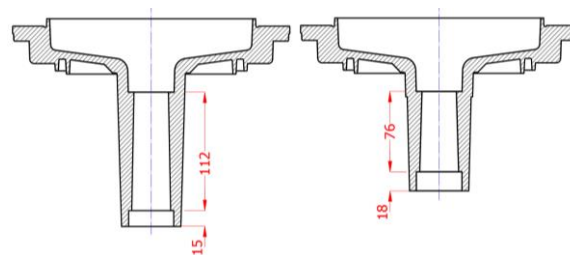


Fig. 2. Changing the length of the casting tube

Table 2.
HPDC process parameters

Temperature in the holding furnace		$710 \pm 10 \text{ }^\circ\text{C}$
Casting (tapping) temperature		$710 \pm 10 \text{ }^\circ\text{C}$
Temperature of mold	Stationary part	$195 \pm 5 \text{ }^\circ\text{C}$
	Moveable part	$195 \pm 5 \text{ }^\circ\text{C}$
Degassing temperature		$720 \pm 5 \text{ }^\circ\text{C}$
Maximum pressure in the chamber		95 MPa
Filling chamber diameter		80 mm
Active chamber length		485 mm
Pressing time		7 s
Rotary degassed with nitrogen		120 s

Table 3.

Changes in maximum piston velocity during the casting process

Marking	V_{max1}	V_{max2}	V_{max3}	V_{max4}
Maximum velocity [$m \cdot s^{-1}$]	2	3	3.6	4

For the melting process we used a melting furnace STRIKO WESTOFEN MHS 750/350 with a holding space capacity of 750 kg. Subsequently, the melt was poured from the furnace into a transport ladle. The melt was automatically degassed with nitrogen by rotary degassing. After degassing, the oxidic membranes were mechanically removed from the surface of the melt, and the melt was then transported to a holding furnace. The casting process took place on a pressure casting machine with a horizontal cold chamber CLH 630.02P.

3. Results

3.1. Makroporosity evaluation

For each casting, three experimental sections were made, marked A-A, B-B and C-C (Figure 3), on which the plane porosity of the experimental castings was evaluated. The samples were ground and scanned part by part with an optical microscope. The parts were then combined using a suitable software in order to create a compact whole. Using the QuickPHOTO INDUSTRIAL 3.2 software, the shapes of the ground sections and pores were contoured by polygons (Figure 4), where their perimeters and areas were calculated.

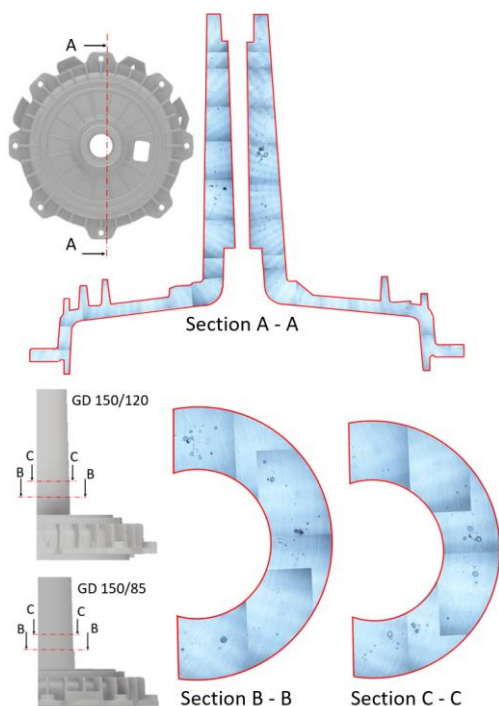


Fig. 3. Placement of control sections on the casting and example of control sections by casting GD 150/120

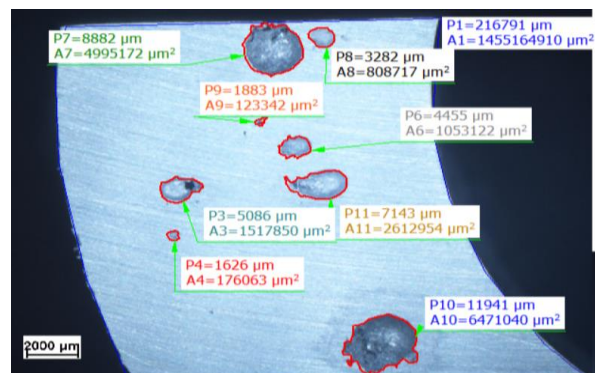


Fig. 4. Evaluation principle in QuickPHOTO INDUSTRIAL 3.2

Macroporosity evaluation of GD 150/120 castings

From the graphs of individual sections, it was possible to conclude that the value of plane porosity changed due to the change of the piston velocity and with a constant tube dimensions. The lowest percentage area porosity was measured on the cross section of the casting (section A-A, Figure 5a). The values on the A-A section did not exceed 1% area porosity and the highest values were measured at a velocity of 2 m/s and 4 m/s). The B-B section already manifests plane porosity over 1% at all velocities (Figure 5b) and the values were kept in a narrow interval (1.03 to 1.38 %). The highest percentage values of porosity occurred in the C-C section, which was made by the external part of the tube (Figure 5c), namely in the range of 1.31% (for the piston velocity 3 m/s) to 3.4 % (for the piston velocity 3.6 m/s). Given this finding, we can conclude that we found a critical spot of the casting where a larger number of pores were present.

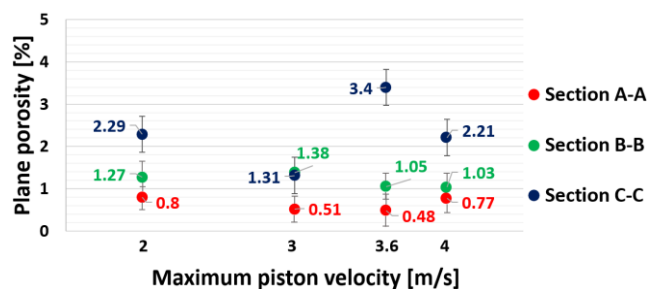


Fig. 5. Resulting porosity of individual sections of GD 150/120 castings

Macroporosity evaluation of GD 150/85 castings

The graphs of the sections (Figure 6) show the evaluation of the plane porosity of the GD 150/85 castings. As with the GD 150/120 castings, the lowest plane (surface) porosity was measured on the A-A section, specifically in a narrow range of 0.45% to 0.63%. In contrast, the largest plane porosity occurred on the B-B section, which represented the lower part of the tube with values ranging from 1.16% to 2.37%. The C-C section manifested a low plane porosity for velocities of 3 and 4 m/s. Regarding the above, the value measured at a maximum piston velocity of 2 m/s was up to 3.37%.

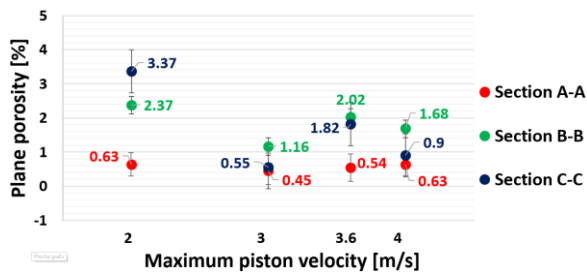


Fig. 6. Resulting porosity of individual sections of GD 150/85 castings

3.2. Brinell hardness

The static hardness test of the experimental castings was performed according to Brinell (in accordance with the EN ISO 6506-1 standard) on 8 samples 4 samples of GD 150/120 castings and 4 samples of GD 150/85 castings, with the press piston velocities). The B-B section was used to evaluate hardness. 30 measurements were performed – 10 measurements in the external, 10 in the middle and 10 in the internal parts of the sample. The individual parts are shown in Figure 7.

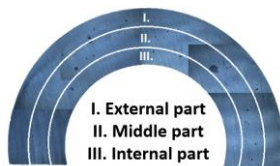


Fig. 7. The sample is divided into individual parts

Graphs of the dependence of the average hardness values on the piston velocities are shown in Figure 8 together with standard deviations. It was also evident from the graphs of average hardness values that the lowest hardness was achieved by the samples of the middle part of the castings, especially at piston velocities of 3 m/s and 3.6 m/s. The middle part was softest due to its greatest distance from the surface and due to the formation thermal nodes in the casting. This region was chosen as the sampling site for microporosity samples. Although the hardness did not change significantly with changing tube dimensions, the values of which were at approximately similar intervals at the same piston velocities, yet the GD 150/85 casting samples manifested a slightly reduced hardness compared to the GD 150/120 samples.

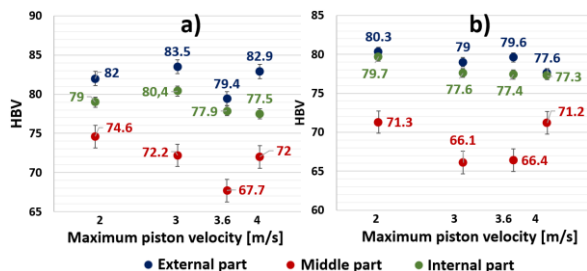


Fig. 8. Graphical representation of the average value of hardness of castings; a) GD 150/120; b) GD 150/85

3.3. Structure evaluation

Samples for experimental examination of the microstructure were taken from the tubular part, the critical site for the formation of porosity. The evaluation took place only on castings with the minimum and maximum piston velocity (2 m/s and 4 m/s).

Microstructure images of GD 150/85 castings

Eutectic silicon in the critical region crystallized mainly as a dark grey needle with varying orientation (so-called unmodified state – hexagonal plate formations), while at a velocity of 2 m/s we could observe clusters of eutectic silicon in a finer and shorter morphology (Figure 9a). The silicon particles, together with a small number of copper-based intermetallic phases (probably Al_2Cu), were evenly distributed in the primary α phase at both velocities. At a microstructure with the piston velocity of 4 m/s, angular eutectic grains were observed in a slightly larger number (Figure 9b) than at a velocity of 2 m/s. It can also be observed that increasing the velocity of the piston leads to a partial refinement of the dendrites of the α phase. Deep etching and mapping showed that for the low piston velocity variant, clusters of smaller lamellae can be observed in a fan-like array (Figure 9c), with increasing velocity the lamellae become thinner and grow in size (Figure 9d). Small polyhedral particles of the Fe-rich phase can be observed in all samples.

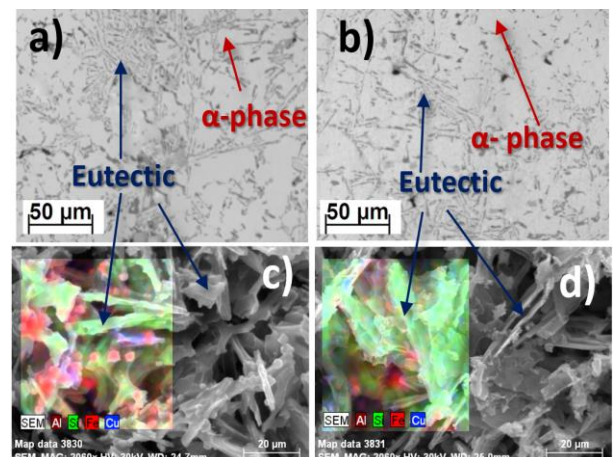


Fig. 9. Microstructure, deep etching and mapping of GD 150/85 castings; a) piston velocity 2 m/s; b) piston velocity 4 m/s; c) piston velocity 2 m/s; d) piston velocity 4 m/s

Microstructure of a GD 150/120 casting

The microstructure (Figure 10) consisted of α phase dendrites, which were documented as brightest spots on the cutting plane. Eutectic silica crystallized at the piston velocity of 2 m/s in the morphology of shorter and thicker needles (Figure 10a,c) compared to the microstructure at a velocity of 4 m/s, when eutectic silicon had the characteristics of longer and thinner needles (Figure 10b,d). Similar to the SB 85 casting, a slight increase in the number of angular eutectic grains and partial refinement of α phase dendrites was observed when the GD 150/120 piston velocity was increased to 4 m/s. Changing the size

of the eutectic Si lamellae by changing the velocity of the piston movement was similar to the GD 150/85 castings.

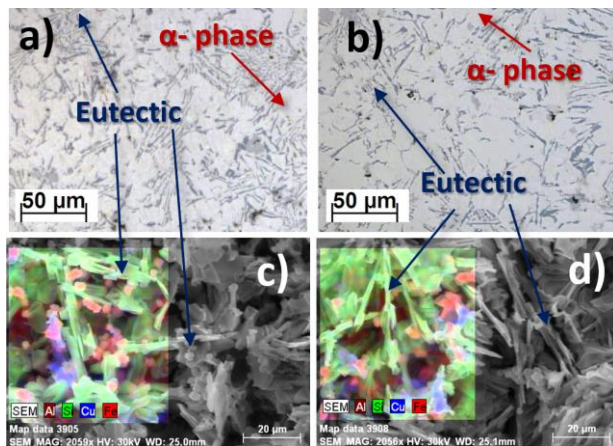


Fig. 10. Microstructure deep etching and mapping of GD 150/120 castings; a) piston velocity 2 m/s; b) piston velocity 4 m/s; c) piston velocity 2 m/s; d) piston velocity 4 m/s

3.4. Microporosity evaluation

As the site for microporosity evaluation we chose the middle region of the tube of the B-B section. A total of 8 samples were created depending on the type of casting and the piston velocity used. Plane microporosity evaluation was performed using the QuickPHOTO MICRO 3.2 software, which has the same interface as the macroporosity evaluation software. In this step, it was important to adjust the correct sensitivity of filters so that only the pore sites were filled (Figure 11a). Based on the values from the five images of each sample, average values were generated and recorded in the graphs. The microporosity graph is shown in Figure 11b, and we can observe that the largest average plane microporosity of the GD 150/120 casting was recorded at the piston velocity of 3.6 m/s. Microporosity values at other piston velocities were very similar, with only a slight difference. The lowest microporosity was measured at the piston velocity of 4 m/s.

The microporosity of GD 150/85 castings at the maximum piston velocities of 2, 3.6 and 4 m/s was slightly reduces compared to GD 150/120 castings. A rapid increase occurred at a velocity of 3 m/s, where the microporosity value was 1.23 %.

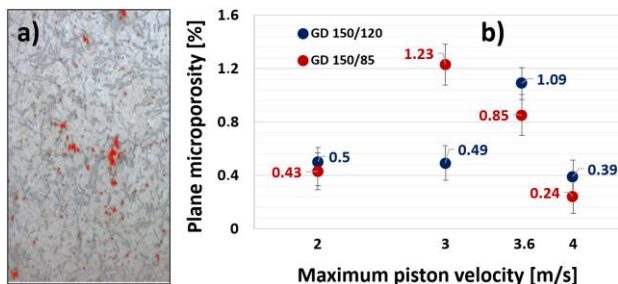


Fig. 11. Microporosity of GD 150/120 and GD 150/85 castings; a) Evaluation principle; b) Graph of the resulting values

4. Discussion

In terms of plane porosity, we can conclude for both types of castings that the optimal piston velocity in the filling chamber was 3 m/s. The maximum piston velocity of 3 m/s caused the optimal dispersive characteristics of the melt flow in the mold cavity. At a piston velocity of 3 m/s, the plane porosity of casting GD 150/120 ranged from 0.51 to 1.38 (for all sections), while by increasing the piston velocity to 3.6 and 4 m/s, the plane porosity slightly decreased, but reached higher values at the C-C sections. For casting GD 150/85, the plane porosity values decreased after increasing the velocity to 3 m/s and remained at approximately the same values even at velocity of 3.6 and 4 m/s. The evaluated decrease in porosity by increasing the maximum velocity of the piston from 2 m/s to a velocity of 3 m/s and higher confirms the results of experiments by Gunasegaram [14], Adamane [15] and Kumar [16] that an increase in the flow rate of the melt led to a decrease in the overall level of porosity in the casting. Wang [17] describes in more detail that as the velocity of the piston increases in the second phase, the filling capacity increases, which leads to a decrease in porosity in the casting. Similar results are reported by Govindarao [18] and Tariq [19], who describes in their work that in order to prevent the formation of large pores caused by contractions and air bubbles, it is necessary to set the maximum velocity of the piston in the filling chamber to the level of 3.5 to 4.5 m/s. When higher speeds than 7 m/s are set, the porosity in the casting increases again.

At the above piston velocity, the melt forms a disperse mixture of molten metal and gases in the mold cavity as a result of the full force of impact on the mold wall. Non-metallic inclusions and gases remain in the casting but are small and evenly distributed in the casting wall. It can equally be concluded that at a piston velocity of 3 m/s the mold filling velocity is already high enough to cause washing away of the initially formed layer (so-called crust) on the mold wall. By reducing the layer on the walls of the mold, the space is expanded and for the strengthening pressure, which is transferred to the solidifying casting with increasing velocity [14].

The highest hardness was at a piston speed of 2 m/s on both tube lengths (74.6 to 82 HBW - GD150/120 and 71.3 to 80.3 HBW - GD150/85). Based on the results, however, it can be concluded that the main cause of the change in hardness was the location of the evaluation, the middle area of the sample clearly had the lowest values with the highest variance (66.1 to 74.6 HBW), the areas near the wall of the casting differed only minimally, which is also confirmed by Gaspar [20] and Yalçın's [21] research.

By observing the microstructure of the castings we found that as the piston velocity increased, there was a slight increase in the number of eutectic grains, which had angular shapes. It was confirmed that at lower piston velocities eutectic silicon crystallized in the form of shorter and thicker needles, whereas at higher velocities this occurred in the form of longer and thinner needles. The results of Kowalczyk's work [22], on the other hand, show that a greater influence on the change in the size of the silicon particles on the change in the wall thickness of the casting. The increase in velocity also caused a refinement of the dendritic grains of the α phase, which confirms the observations of Gunasegaram [14] and Palyga [23], who explains that shear at the gates would break down the larger grains into smaller, rounded forms.

5. Conclusion

The aim of the presented paper is to clarify from experimental castings the influence of the change of the maximum velocity of the pressing piston depending on the different height of the tube on the internal quality of the casting. The following observations follow from the results:

- An increase in the maximum velocity of the piston in the filling chamber from 2 m/s to 3 m/s results in a decrease in porosity in the casting. By increasing the velocity of the piston again to values of 3.6 and 4 m/s, the number of pores in the casting is relatively stabilized.
- Evaluation of the microporosity in the central part of the casting tube showed that the highest values were measured at piston velocity of 3 and 3.6, which had a significant impact on the hardness drop of the castings in the central part of the tube at piston velocity of 3 and 3.6 m/s.
- Increasing the piston velocity has been shown to lead to a refinement of the α phase. Increasing the velocity of the piston also affected the morphology of eutectic Si, where at a velocity of 2 m/s it is characterized by shorter and thicker needles, while at a velocity of 4 m/s it crystallized as longer and thinner needles.
- The increase in the size of the tube when casting GD 150, on the other hand, did not show a significant impact on the internal quality.

References

- [1] Ragan, E. (2007). *Die casting of metals*. Slovakia: Prešov. (in Slovak).
- [2] Cao, L., Liao, D., Sun, F., Chen, T., Teng, Z. & Tang, Y. (2018). Prediction of gas entrapment defects during zinc alloy high-pressure die casting based on gas-liquid multiphase flow model. *The International Journal of Advanced Manufacturing Technology*. 94, 807-815. DOI 10.1007/s00170-017-0926-5.
- [3] El-Sayed, M. A., Essa, K. & Hassanin, H. (2022). Influence of bifilm defects generated during mould filling on the tensile properties of Al-Si-Mg cast alloys. *Metals*. 12(1), 160, 1-15. <https://doi.org/10.3390/met12010160>.
- [4] Timelli, G., & Fabrizi, A. (2014). The effects of microstructure heterogeneities and casting defects on the mechanical properties of high-pressure die-cast AlSi9Cu3(Fe) alloys. *Metallurgical and Materials Transactions A*. 45, 5486-5498. DOI:10.1007/s11661-014-2515-7.
- [5] Lakomá, R., Čamek, L., Lichý, P., Kroupová, I., Radkovský, F., Obzina, T. (2021). Some possibilities of using statistical methods while solving poor quality production. *Archives of Foundry Engineering*. 21(1), 18-22. DOI: 10.24425/afe.2021.136073.
- [6] Martinec, D., Pastircak, R. & Kantorikova, E. (2020). Using of technology semisolid squeeze casting by different initial states of material. *Archives of Foundry Engineering*. 20(1), 117-121. DOI: 10.24425/afe.2020.131292.
- [7] Zhang, Z., Lordan, E., Dou, K., Wang, S. & Fan, Z. (2020). Influence of porosity characteristics on the variability in mechanical properties of high pressure die casting (HPDC) AlSi7MgMn alloys. *Journal of Manufacturing Processes*. 56, 500-509. DOI:10.1016/j.jmapro.2020.04.071.
- [8] Yu, W., Yuan, Z., Guo, Z., & Xiong, S. (2017). Characterization of A390 aluminum alloy produced at different slow shot speeds using vacuum assisted high pressure die casting. *Transactions of Nonferrous Metals Society of China*. 27(12), 2529-2538. [https://doi.org/10.1016/S1003-6326\(17\)60281-4](https://doi.org/10.1016/S1003-6326(17)60281-4).
- [9] Podprocká, R. & Bolibruchová, D. (2017). Iron intermetallic phases in the alloy based on Al-Si-Mg by applying manganese. *Archives of Foundry Engineering*. 17(3), 217-221. DOI: 10.1515/afe-2017-0118.
- [10] Santos, S.L., Antunes, R.A. & Santos, S.F. (2015). Influence of injection temperature and pressure on the microstructure, mechanical and corrosion properties of a AlSiCu alloy processed by HPDC. *Materials & Design*. 88, 1071-1081. DOI:10.1016/j.matdes.2015.09.095.
- [11] Otarawanna, S., Gourlay, C.M., Laukli, H.I. & Dahle, A.K. (2009). The thickness of defect bands in high-pressure die castings. *Materials Characterization*. 60(12), 1432-1441. <https://doi.org/10.1016/j.matchar.2009.06.016>.
- [12] Saeedipour, M., Schneiderbauer, S., Pirker, S., Bozorgi, S. (2015). Prediction of surface porosity defects in high pressure die casting. *Advances in the Science and Engineering of Casting Solidification*. 155-163. DOI: 10.1007/978-3-319-48117-3_19.
- [13] Szalva, P., & Orbulov, I. N. (2020). Influence of vacuum support on the fatigue life of AlSi9Cu3(Fe) aluminum alloy die castings. *Journal of Materials Engineering and Performance*. 29(5), 5685-5695. <https://doi.org/10.1007/s11665-020-05050-y>.
- [14] Gunasegaram, D.R., Finin, B.R., & Polivka, F.B. (2007). Melt flow velocity in high pressure die casting: its effect on microstructure and mechanical properties in an Al-Si alloy. *Materials Science and Technology*. 23(7), 847-856. <https://doi.org/10.1179/174328407X176992>
- [15] Adamane, A.R., Arnberg, L., Fiorese, E., Timelli, G., & Bonollo, F. (2015). Influence of injection parameters on the porosity and tensile properties of high-pressure die cast Al-Si alloys: a review. *International Journal of Metalcasting*. 9(1), 43-53. <https://doi.org/10.1007/BF03355601>.
- [16] Kumar, K.S., Sawale, J.K., & Rao, S. (2013). Study of effect of process parameter setting on porosity levels of aluminium pressure die casting process using Taguchi Methodology. *Journal of Mechanical and Civil Engineering*. 9(4), 12-17. DOI:10.9790/1684-0941217.
- [17] Wang, T., Huang., Fu, H., Yu, K., & Yao. S. (2022). Influence of process parameters on filling and feeding capacity during high-pressure die-casting process. *Applied sciences*. 12, 4757, 1-13. <https://doi.org/10.3390/app12094757>.
- [18] Govindarao, R., Eshwara, K., & Srinivasa Rao, P. (2022). Defect analysis and remedies in the high pressure diecasting process with ADC-12 alloy. *American Journal of Multidisciplinary Research & Development*. 4(7), 1-8.

- [19] Tariq, S., Tariq, A., Masud, M., & Rehman, Z. (2022). Minimizing the casting defects in high-pressure die casting using Taguchi analysis. *Scientia Iranica B*. 29(1), 53-69. DOI: 10.24200/sci.2021.56545.4779.
- [20] Gaspar, S., & Pasko, J. (2019). Plunger pressing speed like the main factor influencing of the mechanical properties of die casting. *MM Science Journal*. 3490-3493 DOI: 10.17973/MMSJ.2019_12_2019029.
- [21] Yalçın, B., Koru, M., Ipek, O., & Özgür, A. E. (2016). Effect of injection parameters and vacuum on the strength and porosity amount of die-casted A380 alloy. *International Journal of Metalcasting*, 11(2), 195-206. <https://doi.org/10.1007/s40962-016-0046-2>.
- [22] Kowalczyk, W., Dánko, R., Górny, M., Kawalec, M., & Burbelko, A. (2022). Influence of high-pressure die casting parameters on the cooling rate and the structure of EN-AC 46000 alloy. *Materials*. 15(16), 5702, 1-16. <https://doi.org/10.3390/ma15165702>.
- [23] Pałyga, Ł., Stachowicz, M., & Granat, K. (2016). Influence of high-pressure die-casting second stage parameter on structure of AlSi9Cu3(Fe) alloy. *Manufacturing Technology*. 16(2), 410-416. ISSN 1213-2489.